# Reaction-Relevant Gold Structures in the Low Temperature Water-Gas Shift Reaction on Au-$CeO_2$

**Weiling Deng,[†] Anatoly I. Frenkel,[‡] Rui Si,[†] and Maria Flytzani-Stephanopoulos*,[†]**

*Department of Chemical and Biological Engineering, Tufts University, Medford, Massachusetts 02155, and Department of Physics, Yeshiva University, New York, New York 10016*

*Received: January 4, 2008; Revised Manuscript Received: May 10, 2008*

Combined in situ X-ray absorption near-edge structure (XANES) and extended X-ray absorption fine structure (EXAFS) studies have been conducted to follow gold structural changes of low-content (<1%Au) gold-ceria catalysts in water-gas shift (WGS) reaction tests at 100 and 200 °C; and after heating the used catalysts in oxygen gas at 150 °C. Gold in the fresh (400 °C-calcined) material was atomically dispersed in cerium oxide. Under WGS reaction conditions, reduction of the oxidized gold species was observed, accompanied by gradual gold aggregation. The Au−Au coordination number is zero for the fresh material, but increases with the reaction temperature, to 6.5 ± 2.4 (after use at 100 °C) and to 8.7 ± 1.5 (after 200 °C) in a gas mixture containing 5% CO- 3% $H_2O$ in helium. The second important parameter is the reaction gas composition which determines the extent of Au−O reduction. The lower the reduction potential of the reaction gas mixture, the more oxidized the gold is in the used catalyst, and the higher its activity. The maximum activity of Au-$CeO_2$ was that of the fully dispersed Au−O−Ce fresh material. Loss of surface oxygen took place during reaction, as measured by $H_2$-TPR of the used samples, and it was commensurate with the activity loss. Attempts to reoxidize and redisperse the gold by heating in oxygen gas at 150 °C were not effective. However, we report here that complete recovery of the surface oxygen amount and redispersion of gold in ceria was possible after a 400 °C- oxygen treatment of both the 100 °C- and 200 °C- used catalyst samples, with concomitant recovery of the initial catalyst activity. These tests were conducted by consecutive $H_2$-TPR/steady-state catalyst activity measurements in the same microreactor.

## Introduction

The water-gas shift (WGS) reaction is a key step in fuel processing to generate high-grade hydrogen for fuel cell and other uses. Highly active and stable WGS catalysts are required for integration in fuel cell systems.[1] The commercially used WGS catalyst in chemical plants, Cu-ZnO, is unsuitable for fuel cell application due to its sensitivity to temperature excursions, air exposure (pyrophoric), and water condensation during shutdown. WGS catalysts based on nanocrystalline cerium oxide (ceria) have been investigated in recent years as alternatives to Cu-ZnO for fuel cell applications.[2–6] They are nonpyrophoric and can be used without activation. The reducibility and catalytic activity of $CeO_2$ are significantly enhanced by the presence of a small amount of a transition metal, which does not have to be a platinum group metal. Platinum was the earliest case demonstrated of a metal additive having a considerable effect on ceria reducibility.[7] However, deactivation of Pt-$CeO_2$ catalysts used in realistic WGS streams[8] and in start−stop operation [9,10] has also been reported. Alternatives to platinum are desirable in order to overcome these problems, and importantly, to reduce the high cost associated with platinum-based catalysts. Nanostructured gold-ceria oxidation catalysts have certain unique properties for low-temperature reformate gas processing.[11] The importance of the cerium oxide structure for the WGS activity of gold-ceria catalyst was identified already in the first report of this catalyst system;[11] and has since been examined in several other publications.[6,12–21]

The literature of fine gold particles supported on reducible oxides has focused on the gold particle size and oxidation state. Accounts of the oxidation state of gold during reaction differ in the literature for the WGS reaction. In transient experiments consisting of injecting CO and $H_2O$ pulses into $H_2$ and He streams, the interfaces of small gold particles with a reduced cerium oxide surface have been identified as important for the WGS reaction; and Au(0) was claimed as the active species.[19] However, nonmetallic gold species, [Au−O−Ce], comprising strongly associated gold cations in ceria, nonleachable by sodium cyanide solution,[6] have been found to have similar or better WGS activity than the parent materials containing a large amount of gold (5wt%), most of which was present as metallic nanoparticles (<5 nm) on ceria.[6,13] The steady-state activities of gold-ceria catalysts reported in the literature are similar. For example, in 1%CO-2%$H_2O$, the WGS reaction rate ($2.8 \times 10^{-7}$ mol$CO_2$/s/$g_{cat}$ at 100 °C) on 2.6 at%Au/$CeO_2$ made by deposition-precipitation (DP) method in ref 18 is very similar to the one reported in refs 11 and 12 ($2.9 \times 10^{-7}$ mol$CO_2$/s/$g_{cat}$ at 100 °C) on 5 wt% Au/$CeO_2$ made by DP as well. However, a strong effect of preparation conditions on the initial activity of gold-ceria has been reported.[17,22–25] Tabakova et al. reported that Au-$CeO_2$ catalysts with gold clusters <1 nm were more active than those containing larger gold clusters for the WGS reaction.[17] This is in agreement with earlier reports from this laboratory [6,13] which showed that in fact the larger particles do not contribute at all, as can be seen by leaching them off the catalyst surface. The interaction with the support and stabilization of

* To whom correspondence should be addressed. Phone: 1-617-627-3048. Fax: 1-617-627-3991. E-mail: mflytzan@tufts.edu.
† Tufts University.
‡ Yeshiva University.

10.1021/jp800075y CCC: $40.75 
Published on Web 07/30/2008

gold on ceria oxygen vacancies has been put forth by DFT calculations to explain the activity of fully dispersed gold in ceria.[26] The importance of a large number of peripheral/interfacial gold atoms has been advocated by Haruta and coworkers.[19] In regard to the charge of gold clusters in ceria, there is conflicting information in the literature, from negative[24] to positive [6,13,26] to neutral.[22,23,27–29] Some of the reported assignments are ambiguous, however, because of the presence of all types of structures of gold (atoms, clusters, nanoparticles) in some of the examined catalysts.

It is clear from reviewing the relevant literature that the properties of Au-$CeO_2$ catalysts for the WGS reaction are not yet fully understood. In view of the importance of this type catalyst as an alternative to Pt-based catalysts, it is of fundamental and practical interest to identify how the strongly interacting gold and ceria species are activated, how they change in response to reaction gas composition and temperature changes, and what role the surface oxygen of ceria plays in the WGS reaction. In reference to the latter, various types of oxygen have been identified on cerium oxide,[30–34] from weakly bound adsorbed oxygen to surface capping oxygen to lattice oxygen, depending on the operating temperature. In the presence of gold, surface reduction of ceria by carbon monoxide begins below room temperature, and several surface oxygen species of different reducibility are present.[6] Cyclic CO-TPR followed by reoxidation has demonstrated excellent stability of the redox properties of these surfaces.[35]

In situ characterization of gold-ceria catalysts by X-ray absorption near-edge structure (XANES) and extended X-ray absorption fine structure (EXAFS) is a powerful tool to investigate the functioning catalyst structure during the reaction. For the CO oxidation, it has been reported that the catalytic activity is proportional to the EXAFS coordination number of Au−O bond in Au-$CeO_2$ catalysts.[20] A combined EXAFS and DFT study of Au-$CeZrO_4$ for the WGS reaction has suggested that metallic gold clusters containing about 50 atoms in intimate contact with the support provide the active sites for the reaction.[28] This conclusion was based on the observation that after 100 °C- or 350 °C -WGS reaction, the predominant species was zerovalent gold in the Au-$CeZrO_4$ catalyst. However, in a more recent paper,[36] dramatic deactivation of the same Au-$CeZrO_4$ catalyst after use in the WGS reaction was reported. There appears to be a correlation between $Au^0$ enrichment and catalyst deactivation. In another EXAFS study, it has been suggested that at temperatures above 250 °C, the WGS reaction occurs at the gold-ceria interface, the active phase involving gold nanoparticles smaller than 2 nm and oxygen vacancies.[29] It is noteworthy that in both of the above studies, the as-prepared catalysts contained gold nanoparticles and subnanometer size gold clusters. It was thus, impossible to discriminate between the different phases, evaluate the activity of each, and/or follow the structural evolution of the minor phase (dispersed gold atoms/clusters) with the reaction conditions.

Starting from a fully dispersed gold state, where no Au−Au, but only Au−O coordination is seen by EXAFS, would make the results less ambiguous, and would allow the structural evolution under reaction conditions to be correlated with the enhancement or loss of activity. The work reported here aimed at achieving this specific objective. To this end, we used catalysts that contained initially no gold nanoparticles, but only bound, oxidized gold species, [Au−O−Ce], as characterized by XANES and XPS. This allowed us to examine the gold structure evolution under different WGS reaction conditions, and compare it to the corresponding catalytic activity.

## Experimental Section

One of the low-content gold-ceria samples, 0.75Au$CeO_2$, was prepared by the urea gelation coprecipitation (UGC) method[35] by mixing an aqueous solution of $HAuCl_4 \cdot 3H_2O$ and $(NH_4)_2Ce(NO_3)_6$ with urea under boiling conditions (~95 °C) for more than 8 h under intermittent addition of water. The slow decomposition of urea allows a more homogeneous precipitation than carbonate or hydroxide coprecipitation methods. After aging to gel state, the precipitate was washed/filtered 3 times with boiling D.I. water, dried at 100 °C for10 h, and calcined in static air at 400 °C for 10 h. A slow heating rate (2 °C/min) was used until the final calcination temperature was reached. A second low content gold-ceria (0.5AuCe(La)Ox) was prepared by using a 2%NaCN solution at pH 12 to leach out all the weakly bound gold from a 400 °C-calcined 5%AuCe(La)Ox. The latter was prepared by deposition-precipitation (DP) from a gold precursor solution on a Ce(La)Ox support, containing 10 atom % La, as described elsewhere.[6,13] Cyanide leaching removed ~90% of the gold from the parent sample, but no other component was leached out, as checked by ICP. Leached samples were washed by deionized water three times; then dried in a vacuum oven for 10 h, and heated in air at 400 °C for 2 h. Selected used materials after the WGS reaction were treated with the 2% NaCN solution to check how much gold could be further stripped off, which can be used as an indication of the extent of loss of the gold-ceria interaction.

All reagents used in catalyst preparation were of analytical grade. The samples reported here are denoted as a$AuCeO_2$ or aAuCe(La)Ox, in which a is the gold content in atomic percent and Ce(La)Ox is a 10 at %La-doped ceria. The samples referred as "fresh" were in the as prepared state after calcination in static air at 400 °C.

Bulk elemental analysis of the catalyst samples was performed by inductively coupled plasma optical emission spectrometry (ICP-OES, Leeman Laboratories Inc.). Scanning transmission electron microscopy (STEM) analyses were performed in a Vacuum Generators HB603 STEM equipped with an X-ray microprobe of 0.14nm optimum resolution for Energy Dispersive X-ray Spectroscopy (EDX). The sample powder was dispersed on a copper grid coated with a carbon film and elemental maps were obtained on a 128 × 128 data matrix. XPS analysis was performed on a Kratos AXIS Ultra Imaging X-ray Photoelectron Spectrometer with a resolution of 0.1 eV used to determine the oxidation state of gold in selected catalysts. Samples were in powder form and were pressed on a double-side adhesive copper tape. All measurements were carried out at room temperature without any sample pretreatment. An Al Kα X-ray source was primarily used in this work. The X-ray generator power was typically set at 15 kV and 10 mA. All binding energies were adjusted to the C 1s peak at 285 eV. An adjacent neutralizer was used to minimize the static charge on the samples.

XANES was employed to examine the oxidation state of various gold-ceria materials under different treatments. In-situ EXAFS of selected gold-ceria samples took place under the WGS reaction and in reoxidation conditions. The spectra were collected using the beam line X18B of the National Synchrotron Light Source (NSLS) at Brookhaven National Laboratory. For in situ EXAFS measurements, the sample was loaded into a polyimide tube microreactor (0.123 in. I.D.) with quartz wool blocking both ends of the catalyst bed to keep the catalyst powder in place, only allowing the reaction gas mixture to flow through the tube. Water vapor (at ~3 mol%) was introduced into the reactor by saturation of the CO/He gas stream flowing

through a water bubbler kept at room temperature. The reactor temperature was controlled by a temperature controller with a J type thermocouple in contact with the catalyst. The reactor tube was held inside an aluminum block holder equipped with heating rods. The EXAFS spectra were taken in the fluorescence mode. The 13-channel Ge detector was placed at 90° with respect to the incident beam to minimize elastic scattering. The reactor tube was placed at 45° both to the incident beam and the Ge detector. The X-ray absorption edge energy was calibrated by assigning the 11919 eV to the first inflection point in the standard Au foil XANES. The reported XANES data are the averages of three scans (lasting approximately 35 min/scan). No changes were detected between the first and the last scan. The reported EXAFS data were the averages of over fifteen scans collected after cooling the sample down to room temperature following various treatments. The data were processed by the Athena and Artemis programs.[37,38]

Temperature-programmed reduction by hydrogen ($H_2$-TPR) was conducted in a Micromeritics Pulse ChemiSorb 2705 instrument equipped with a thermal conductivity detector to detect $H_2$ consumption after condensing out the produced water. The selected catalyst samples in fine powder form (50 mg) were heated at a rate of 5 °C/min from room temperature to 400 °C in a 20% $H_2/N_2$ (20 $cm^3$/min (NTP)) gas mixture. In-situ WGS/TPR experiment was conducted by coupling the TPR instrument (Micromeritics 2705) with a mass spectrometer (MKS-model RS-1). The WGS reaction was run over a 200 mg catalyst sample in a 5%CO-3%$H_2O$−He gas mixture at the desired temperature for 1 h with on line measurement of the CO, $CO_2$, $H_2$ concentrations by the mass spectrometer. After reaction, the used catalyst was treated either at room temperature in helium or at 400 °C in a 20% $O_2$/He gas mixture, followed by $H_2$-TPR, without exposure to the ambient.

Separate WGS reaction tests were conducted at atmospheric pressure with the catalyst in powder form (<150 $\mu$m). A quartz tube (O.D. = 1 cm) with a porous quartz frit supporting the catalyst was used as a packed-bed flow reactor. Water was injected into the flowing gas stream by a calibrated syringe pump and vaporized in the heated gas feed line before entering the reactor. A condenser filled with ice was installed at the reactor exit to collect water. The feed and product gas streams were analyzed by a HP-6890 gas chromatograph (GC) equipped with a thermal conductivity detector (TCD). A Carbosphere (Alltech) packed column (6 ft × 1/8 in.) was used to separate CO, $H_2$ and $CO_2$. No methane was produced under any of the operating conditions used in this work.

## Results and Discussion

In Figure 1, the high white line intensity XANES of the fresh 0.5AuCe(La)Ox material (line a) indicates a high density of d-holes in Au, consistent with its richer O environment relative to the other samples. This observation is consistent with the R-space EXAFS data in Figure 2. The FEFF6 theory[39] was used to fit the Au−O, Au−Au and Au−Ce interactions in all the samples.[37,38] The EXAFS fitting was performed based on a substitution model, in which Au was placed into a $Ce^{4+}$ site in $CeO_2$ structure. The best fit values of the coordination number CN, shell distance R, and the mean squared relative deviation (also known as EXAFS Debye−Waller factors) $\sigma^2$ for Au−O and Au−Au bonds are listed in Table 1. The coordination number of Au−O1 at the shorter distance for the fresh catalyst was 2.7 ± 0.9. The first shell radial distance of Au−O1 at 1.97 Å indicated the direct bonding between Au and O. The longer Au−O2 distance at 3.3 Å implies nonbonding interactions of

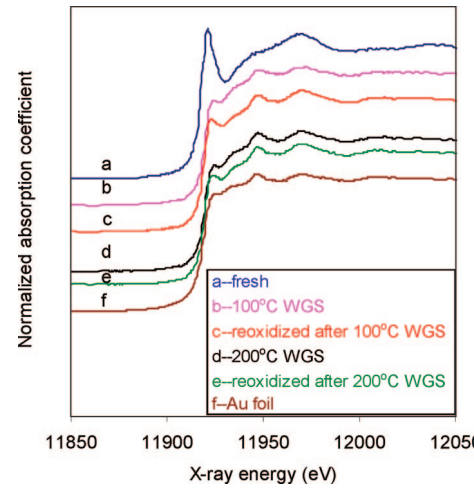


**Figure 1.** XANES spectra of 0.5AuCe(La)Ox during WGS reaction in 5%CO-3%$H_2O$−He and reoxidation in 5%$O_2$/He at 150 °C.

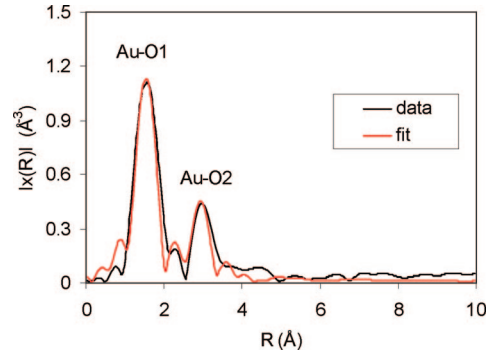


**Figure 2.** EXAFS data (black) and fit (red) of fresh 0.5AuCe(La)Ox in R space.

gold with oxygen of the ceria support surface.[20] No Au−Au or Au−Ce contributions within the first 3.5 Å could be detected. The presence of positively charged Au in the fresh 0.5AuCe(La)Ox catalyst is corroborated by the XPS analysis shown in Figure 3. The energies at 83.5 and 87.2 eV are assigned to $Au^{1+}$ while 84.5 and 88.2 eV are assigned to $Au^{3+}$ binding energies.[13,35] Therefore, no $Au^0$ was present in the fresh 0.5AuCe(La)Ox material as confirmed by both the EXAFS/XANES and XPS analyses.

The WGS reaction was conducted over 0.5AuCe(La)Ox at 100 °C in a gas mixture of 5%CO-3%$H_2O$−He at a total flow rate of 10 mL/min. XANES spectra were taken after 1 h reaction as shown in Figure 1, line b. The decreased white line intensity shows that the O-rich environment for the fresh sample no longer exists. EXAFS spectra were taken when the sample was cooled down to room temperature. Some of the oxidized gold was reduced after this test, as depicted by the lowering of the Au−O coordination number (Table 1). The Au−Au contribution is dominant as shown in the R-space (Figure 4a). The two large peaks labeled as Au−Au are due to a single Au−Au path contribution. This splitting is due to Ramsauer−Townsend resonance at a single energy in the backscattering amplitude of Au. In our fitting trials, adding Au−Ce into the fit improves the result. Without Au−Ce, the fourth peak intensity in the R-space figure is much lower than the experimental data. However, due to the noise level in the long R range above 3 Å, an accurate determination of Au−Ce coordination number can not be achieved. The Au−Ce distance at 3.83 Å (not shown) obtained from the fitting was consistent with a DFT calculation by Tibiletti et al.[28] In their calculation, the Au−Ce distance was

**TABLE 1: Numerical Results (Coordination Numbers CN, Distances R, Debye−Waller Factors $\sigma^2$) for Au−O and Au−Au Bonds in the 0.5AuCe(La)Ox Samples**

| | Au−O [a] | | | Au−Au | | |
|---|---|---|---|---|---|---|
| sample | CN | R (Å) | $\sigma^2$ (Å$^2$) | CN | R(Å) | $\sigma^2$ (Å$^2$) |
| 0.5AuCL, fresh | 2.7 ± 0.9 | 1.97 ± 0.03 | 0.000 ± 0.005 | 0 | | |
| 100 °C WGS | 0.4 ± 0.3 | 1.99 ± 0.08 | 0.000 ± 0.004 | 6.5 ± 2.4 | 2.85 ± 0.03 | 0.009 ± 0.004 |
| 150 °C $O_2$, after 100 °C WGS | 0.7 ± 0.4 | 1.95 ± 0.04 | 0.000 ± 0.002 | 6.6 ± 1.6 | 2.883 ± 0.002 | 0.005 ± 0.003 |
| 200 °C WGS | 0.4 ± 0.1 | 1.94 ± 0.03 | 0.000 ± 0.004 | 8.7 ± 1.5 | 2.855 ± 0.009 | 0.008 ± 0.002 |
| 150 °C $O_2$, after 200 °C WGS | 0.4 ± 0.3 | 1.96 ± 0.05 | 0.000 ± 0.007 | 8.7 ± 1.5 | 2.852 ± 0.03 | 0.008 ± 0.002 |

[a] The results reported here are for the shortest Au−O distance only.

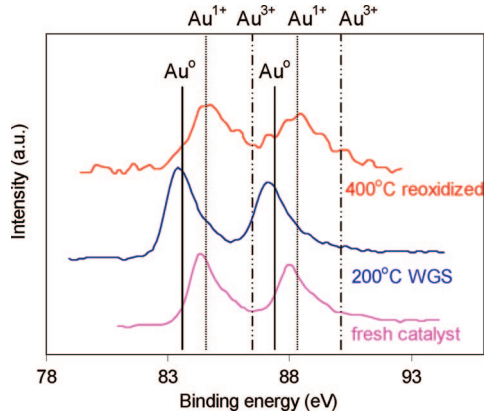


**Figure 3.** XPS spectra of Au 4f for the fresh, 200 °C WGS used and 400 °C reoxidized 0.5AuCe(La)Ox.

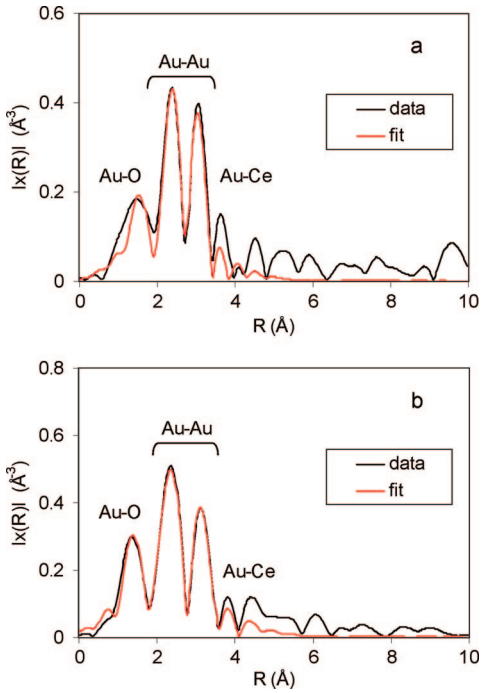


**Figure 4.** EXAFS data (black) and fit (red) in R-space of 0.5AuCe(La)Ox: (a) after 1 h WGS reaction at 100 °C; (b) 1 h 150 °C reoxidation in 5%$O_2$ after (a).

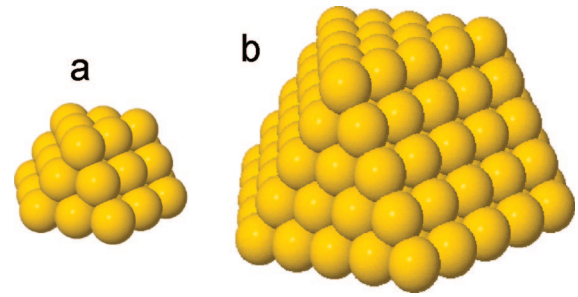


**Figure 5.** Models of Au nanoparticles based on (a) truncated cuboctahedron with 37 Au atoms (3 Au atoms on each edge); (b) truncated cuboctahedron with 185 Au atoms (5 Au atoms on the each edge). Models are derived from ref 40.

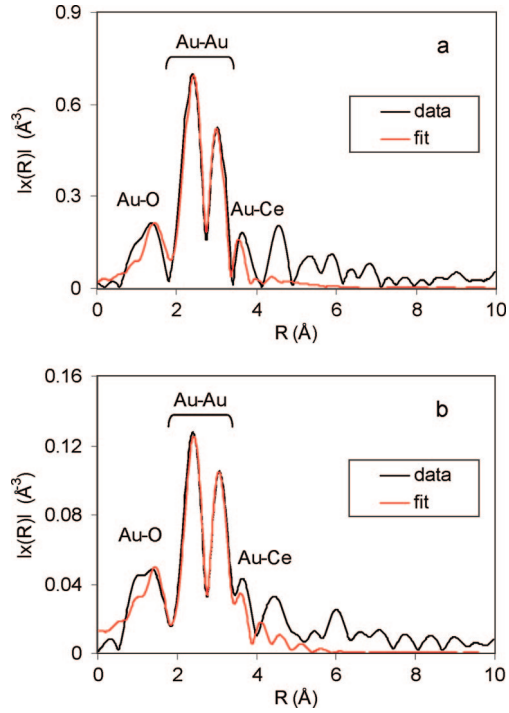


**Figure 6.** EXAFS data (black) and fit (red) in R-space of 0.5AuCe(La)-Ox: (a) after 1 h WGS reaction at 200 °C; (b) 1 h 150 °C reoxidation in 5%$O_2$ after (a).

at ~3.88 Å, if Au was assumed to fill a cerium ion vacant site (on the $CeO_2$ (111) plane). The similarity of these values supports the substitution model that we used for the EXAFS fitting.

As can be seen in Table 1, the coordination number of Au−O decreased from 2.7 ± 0.9 for the fresh catalyst to 0.4 ± 0.3 after 100 °C- WGS reaction, while the Au−Au coordination number was stabilized at 6.5 ± 2.4, i.e., much smaller than in pure Au (12), with a shell distance of 2.85 ± 0.03 Å. These results are consistent with formation of gold clusters during the reaction at 100 °C. Thus, the sample has a mixture of Au clusters and Au atoms embedded in ceria lattice. Figure 5a shows a model used to simulate the structure of an fcc, hemispherical (truncated by a (111) plane) cuboctahedral gold cluster of 37[40] atoms formed after the 100 °C -WGS reaction. The coordination number was calculated as 6.97 in the structure shown in Figure 5a assuming 3 Au atoms on each edge. The particle diameter was estimated as 1.15 nm, setting the nearest neighbor distance at 2.87 Å as in pure Au. This demonstrates that the 0.5AuCe(La)Ox

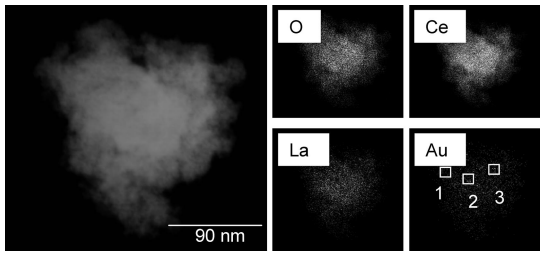


**Figure 7.** STEM/EDX of 0.5AuCe(La)Ox after 1 h 200 °C WGS reaction in 5%CO-3%$H_2O$−He.

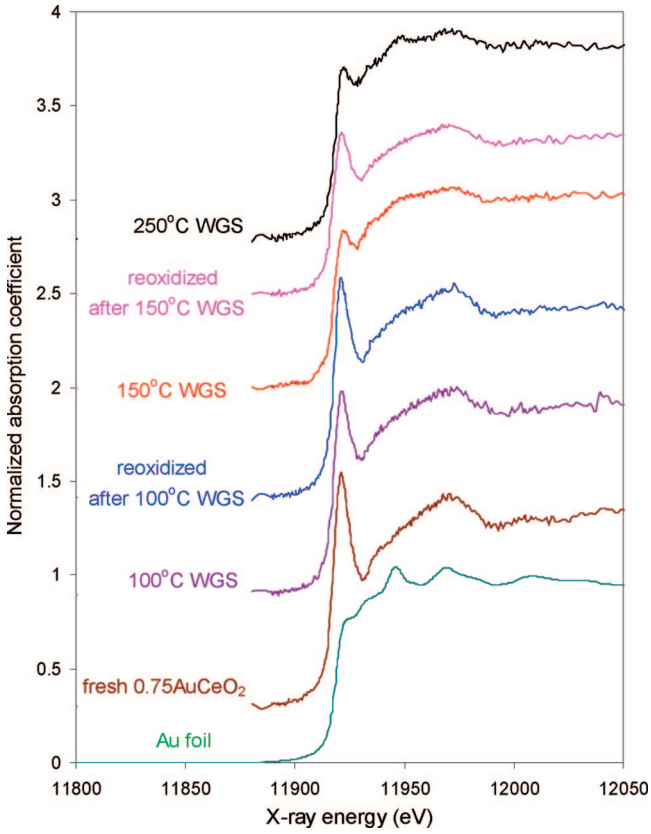


**Figure 8.** XANES spectra of 0.75$AuCeO_2$ during WGS reaction in 1%CO-3%$H_2O$−He and reoxidation in 5%$O_2$/He at 150 °C.

**TABLE 2: 0.5AuCe(La)Ox in the WGS Reaction and after NaCN Leaching of the Used Catalysts**

| | 100 °C CO conversion (%) | 200 °C CO conversion (%) | Au concentration (at.%) |
|---|---|---|---|
| fresh catalyst | 15.7 | 44.8 | 0.50 |
| 100 °C used, then NaCN leached | 11.2 | | 0.39 |
| 200 °C used, then NaCN leached | | 26.8 | 0.22 |
| 100 °C used, followed by 400 °C oxidation, then NaCN leached | | | 0.47 |
| 200 °C used, followed by 400 °C oxidation, then NaCN leached | | | 0.35 |

catalyst after 100 °C- WGS reaction should not contain gold clusters larger than 1nm in diameter. From the STEM/EDX analysis (Supporting Information) of this used material, the Au elemental map does not show any coarsening of gold clusters, which is consistent with the results obtained from Figures 4a and 5a. After the EXAFS spectra were taken at room temperature, the used material was heated to 150 °C in 5%$O_2$ gas and kept at it for 1 h. Partial oxidation was observed by the small increase of the white line intensity in Figure 1, line c. The analysis of the EXAFS data shown in Figure 4b clearly indicates the combined contribution from Au−O, Au−Au and Au−Ce. As shown in Table 1, the coordination number of Au−O increased from 0.4 ± 0.3 to 0.7 ± 0.4 after this oxidation, implying that partial reoxidation had taken place, while some irreversible structure change of gold must have occurred during the reaction.

In a separate experiment, a fresh catalyst was loaded into the polyimide reactor and the WGS reaction was run at 200 °C for 1 h. The XANES of the used material is shown in Figure 1, line d. A higher reduction extent of gold was clearly observed after the 200 °C-WGS reaction than after 100 °C. The coordination number of Au−Au is 8.7 ± 1.5 (Table 1) from the fitting result in Figure 6a, higher than the 100 °C- used sample (6.5 ± 2.4). Hence, the Au−Au coordination number is a function of the reaction temperature. The reduction extent of gold from $Au^{\delta+}$ to $Au^0$ is increased with the WGS reaction temperature, and leads to partial activity loss, as will be discussed below. The Au−O contribution is the same as the sample used in 100 °C reaction. Reoxidation by 5%$O_2$/He at 150 °C of the 200 °C- used material did not increase the Au−O contribution and the coordination number of Au−Au was 8.7 ± 1.5, the same as in the used material. The gold structure is thus quite stable after the 200 °C-reaction.

The reoxidation extent of $Au^0$ to $Au^{\delta+}$ after WGS reaction is controlled by the close interaction of gold and ceria. As discussed above, when subjected to 150 °C oxidation, the Au−O contribution in gold-ceria catalyst is partially recovered for the 100 °C WGS-used catalyst. However, there is no significant Au−O contribution change for the 200 °C WGS-used catalyst after the same oxygen treatment. This observation is consistent with the previous report by Tibiletti et al.,[28] in which ∼15% reoxidation of Au° was observed after air treatment for the 100 °C WGS-used catalyst while no oxidation was found for their 350 °C WGS-used catalyst. Not only the gas composition changes the gold oxidation state during the WGS reaction,[13] but the reaction temperature also dictates the extent of $Au^{\delta+}$/$Au^0$. As reported by Wang et al. earlier,[29] at reaction temperatures above 200 °C, XANES spectra of the gold-ceria (doped with gadolinia) catalyst indicated the $AuO_x$ in the catalyst was fully reduced in 5%CO-3%$H_2O$−He. The assignment of $Au^0$ as the active state in the working catalyst is speculative, however, since the XANES data were not compared to the catalyst activity with time-on-stream at the same reaction conditions.

Figure 5b shows a model for the estimation of gold particle size in the 200 °C- used catalyst. This model corresponds to a truncated cuboctahedron structure which contains 185 Au atoms, a cluster with 5 Au atoms on each edge. The calculated coordination number of Au−Au is 8.89 with an estimated particle size of 2.3nm. Consistently, the 200 °C- used catalyst shows special features in the elemental maps of STEM/EDX analysis as shown in Figure 7. In the selected 3 spots in the Au elemental map, the Au concentration is 2.2, 1.0, 3.4 at%, slightly higher than the average concentration (0.5 atom %) in this sample. This is an indication of agglomeration of gold due to the 200 °C- WGS reaction. However, this gold cluster/particle coarsening is reversible. Corroborating evidence to support this argument was derived from a reoxidation experiment performed

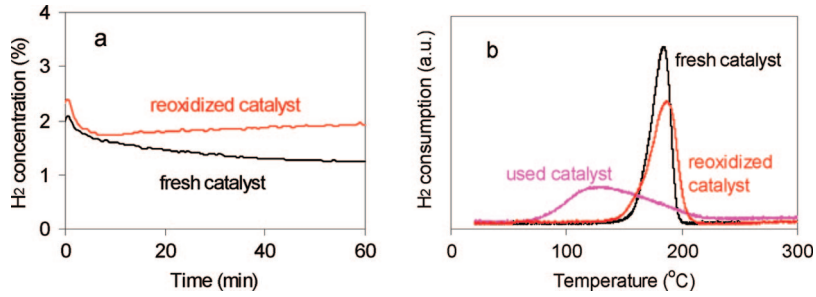


**Figure 9.** In situ WGS/$H_2$TPR over 0.5AuCe(La)Ox catalyst. (a) Hydrogen production measured by mass spectrometry during the 200 °C- WGS reaction in a gas mixture of 5%CO-3%$H_2O$−He (200 mg catalyst, gas flow rate 20 mL/min); (b) $H_2$-TPR profiles for the fresh, used and reoxidized catalysts. Reoxidation condition: 400 °C in 20%$O_2$ for 1 h after the 200 °C- WGS reaction. $H_2$-TPR test condition: 20%$H_2$/$N_2$, flow rate 20 mL/min, heating rate: 5 °C/min.

**TABLE 3: Hydrogen consumption in $H_2$-TPR tests of 0.5AuCe(La)Ox after various treatments**

| sample | $H_2$ consumption ($\mu$mol/$g_{cat}$) |
|---|---|
| fresh | 634 |
| 100 °C WGS | 497 |
| 150 °C $O_2$ after 100 °C WGS | 427 |
| 200 °C WGS | 443 |
| 150 °C $O_2$ after 200 °C WGS | 484 |
| 100 °C WGS, then leached | 466 |
| 200 °C WGS, then leached | 447 |

in conjunction with a WGS/$H_2$-TPR test, as will be discussed below. On the other hand, these agglomerated gold particles/clusters are not crystalline, as confirmed by the HRTEM picture taken for the 200 °C- used sample (Supporting Information). All lattice fringes belong to ceria crystallites, not to gold crystallites, by looking into the *d*-spacing.

The oxidation state of gold during the WGS reaction is actually controlled by the gas composition. In a practical reformate gas mixture (11%CO-26%$H_2O$-26%$H_2$-7%$CO_2$), the Au−Au coordination number of 0.5AuCe(La)Ox is 6.0 ± 2.9, even after testing at 350 °C (not shown), which corresponds to ~1 nm particle size. In a more oxidizing condition, such as the 1%CO-3%$H_2O$−He shown in Figure 8, a higher amount of oxidized gold species was retained determined by the Au white line intensity for 0.75Au$CeO_2$, which is consistent with our previous findings.[13] Indeed, highly reducing WGS gas compositions cause the formation and growth of metallic Au nanoparticles, and this is accompanied by loss of catalyst activity.[13,41] Conversely, we have reported that at any temperature, deactivation is suppressed in fuel gases with higher oxygen potential.[10]

To investigate the reduction of ionic gold in the 0.5AuCe(La)Ox catalyst during the WGS reaction, two samples were tested ex situ in the flow quartz reactor in 5%CO-3%$H_2O$−He (same gas composition as in the EXAFS experiments) at 100 and 200 °C to measure the CO conversion at each temperature. Results are shown in Table 2. After reaction at each temperature, the used material was treated with a 2%NaCN solution to remove any gold species which had lost their interaction with ceria due to reaction. It was found (by ICP) that 20% of gold could be leached from the 100 °C- used catalyst, while 56% of gold was removed from the 200 °C- used catalyst. The loss of bound gold resulted in activity drop reflected by lower CO conversion.

As discussed in the Supporting Information, a 150 °C- reoxidation can not restore the gold ion-ceria interaction in the reaction-used catalyst. A 400 °C- reoxidation is needed to effectively do this. Consecutive WGS/$H_2$-TPR tests (Figure 9) were then run to show that redispersion of gold is accompanied by recovery of the activity and recovery of the surface oxygen amount. As can be seen in Figure 9b, after 200 °C- WGS reaction in a gas mixture of 5%CO-3%$H_2O$−He, the reduction temperature shifted to as low as 50 °C and the hydrogen consumption in TPR decreased to 502 $\mu$mol/g from 634 $\mu$mol/g in the fresh material. This correlates well with the WGS activity loss shown in Figure 9a. The hydrogen produced by reaction dropped from 40% to 25% after 1 h reaction at 200 °C. After treatment in 20%$O_2$/He gas at 400 °C for 1 h, the $H_2$-TPR profile of the used catalyst was almost the same as the fresh material, and the surface oxygen amount was mostly recovered, as measured by a hydrogen consumption of 614 $\mu$mol/g. Thus, gold nanoparticles formed during reaction can be redispersed in ceria after high-temperature oxidation; and the process is fully reversible. The reoxidation of the used material also leads to the recovery of the initial catalyst activity as seen in Figure 9a.

Redispersion of Au in ceria is corroborated by XPS analyses of the 200 °C- used and 400 °C- reoxidized samples. By peak deconvolution of the used sample in Figure 3, after the 200 °C- WGS reaction, ~53% of gold was converted to $Au^0$, while ~47% remained oxidized. However, after 400 °C- oxidation for 1 h, most of the gold was oxidized, with a negligible amount of $Au^0$ present. The used catalyst was exposed to ambient conditions before the XPS measurement, but this does not affect the gold oxidation state.[41] The room temperature reoxidation of the reduced gold-ceria catalyst surface reported in ref 35 is that of ceria, not gold.[41]

The surface oxygen amounts measured by $H_2$-TPR over differently treated samples can be found in the Support Information (Figure S4, Table S1). The reducibility of the fresh and used materials was not the same and the amount of oxygen reduced was different. The used materials, reoxidized at 150 °C after WGS reaction, showed the typical more reducible oxygen attributed to the presence of zerovalent gold particles,[6] as indicated by the low-temperature reduction of oxygen beginning at 50 °C due to spillover effect of hydrogen from the metal to ceria.[42] In addition, the total amount of surface oxygen reduced was lower than in the fresh materials. The drop in surface oxygen amount is related to the observed lower activity for the WGS reaction.

Reoxidation of the used materials by oxygen at 400 °C restored the catalyst oxygen storage capacity. NaCN leaching of the 400 °C- reoxidized materials (Figure S5) removed only 6% of the original 0.5 atom % gold in the 100 °C- used sample, rather than the 20% gold which was leachable after the 100 °C- WGS reaction. The ICP analyses after such treatments of various samples are also listed in Table 2. For the 200 °C- used sample, NaCN removed ~50% of gold after the reaction, while 400 °C- reoxidation was able to restore most of the dispersed [$Au_n$−O-Ce] species, with 70% of the initial gold now being strongly bound in ceria.

The surface gold atoms/clusters are indeed in a very dynamic state. It was recently reported that upon exposure to the electron beam for a few minutes during the TEM observation, nanometer-size Au particles easily diffuse into the $CeO_2$ surface and subsurface layers.[43] In this work, we have observed how redox treatments can affect the mobility of gold in ceria. The redispersion of gold by oxygen treatment at high temperatures is important both from a fundamental and a practical viewpoint. As reported by Tibiletti et al.,[28] 150 °C air oxidation was able to reoxidize ~15% of gold after 100 °C -use in the WGS reaction, while this treatment was inadequate to reoxidize any of gold after 350 °C -WGS reaction. In a DRIFTS study of $Au/CeO_2$ catalyst during CO oxidation by Romero-Sarria et al.,[44] a change of gold dispersion (indicated by intensity of CO adsorption band) was observed by deep reduction of the surface and migration of oxygen atoms from the bulk to the surface. Similar evaluation under water-gas shift conditions, followed by oxygen treatments at various temperatures would be useful in future work to elucidate the mechanism of gold redispersion.

## Conclusion

Gold changes from a fully cationic state in fresh low-content $Au-CeO_2$ samples to a partially reduced state after WGS reaction at temperatures as low as 100 °C. The Au−Au coordination number increases with reaction temperature, from $6.5 \pm 2.4$ at 100 °C to $8.7 \pm 1.5$ at 200 °C- reaction with a gas mixture of $5\%CO\text{-}3\%H_2O-He$. A gas with a lower reduction potential causes less reduction of gold. Hence, the oxidation of gold is controlled by the reaction gas composition. While all of these states represent a "working" catalyst, the activity of each state is different; the fully dispersed fresh catalyst being the most active.

The loss of surface oxygen in the reaction- used samples was found to correlate with gold aggregation and catalyst activity loss. We report here for the first time that this is a reversible structural change. Redispersion of gold on the ceria surface was observed after 400 °C reoxidation of the used catalyst, accompanied by activity recovery. These results can guide the design of gold/ceria catalysts, and of the processing conditions, e.g. addition of small amounts of oxygen in the reformate gas, to control deactivation and prolong the catalyst lifetime.

**Acknowledgment.** The financial support of this work by the NSF Nanotechnology Interdisciplinary Research Team (NIRT) Grant No. 0304515 and by DOE, Basic Energy Sciences, Hydrogen Fuel Initiative Grant No. DE-FG02-05ER15730 is gratefully acknowledged. A.I.F. acknowledges the U.S. DOE Grant No. DE-FG02- 03ER15476 for support. W.D. is thankful for the travel assistance and on site support provided by the Synchrotron Catalysis Consortium (U.S. DOE Grant No. DE-FG02- 05ER15688). The NSLS is supported by the Divisions of Chemistry and Materials Science of the U.S. Department of Energy. We thank Dr. Anthony Garratt-Reed of MIT for his assistance with the STEM/EDX analyses.

**Supporting Information Available:** This information is available free of charge via the Internet at http://pubs.acs.org.

## References and Notes

(1) Farrauto, R. J. *Appl. Catal., B* **2005**, *56*, 3.
(2) Bunluesin, T.; Gorte, R. J.; Graham, G. W. *Appl. Catal., B* **1998**, *15*, 107.
(3) Hilaire, S.; Wang, X.; Luo, T.; Gorte, R. J.; Wagner, J. *Appl. Catal., A* **2001**, *215*, 271.
(4) Swartz, S. L.; Seabaugh, M. M.; Holt, C. T.; Dawson, W. J. *Fuel Cell Bull.* **2001**, *30*, 7.
(5) Li, Y.; Fu, Q.; Flytzani-Stephanopoulos, M. *Appl. Catal., B* **2000**, *27*, 179.
(6) Fu, Q.; Saltsburg, H.; Flytzani-Stephanopoulos, M. *Science* **2003**, *301*, 935.
(7) Yao, H. C.; Yu Yao, Y. F. *J. Catal.* **1984**, *86*, 254.
(8) Zalc, J. M.; Sokolovskii, V.; Loffler, D. G. *J. Catal.* **2002**, *206*, 169.
(9) Liu, X.; Ruettinger, W.; Xu, X.; Farrauto, R. *Appl. Catal., B* **2005**, *56*, 69.
(10) Deng, W.; Flytzani-Stephanopoulos, M. *Angew. Chem., Int. Ed.* **2006**, *45*, 2285.
(11) Fu, Q.; Weber, A.; Flytzani-Stephanopoulos, M. *Catal. Lett.* **2001**, *77* (1−3), 87.
(12) Fu, Q., Ph. D. Dissertation, Department of Chemical and Biological Engineering, Tufts University, 2004.
(13) Fu, Q.; Deng, W.; Saltsburg, H.; Flytzani-Stephanopoulos, M. *Appl. Catal., B* **2005**, *56*, 57.
(14) Andreeva, D.; Idakiev, V.; Tabakova, T.; Ilieva, L.; Falaras, P.; Bourlinos, A.; Travlos, A. *Catal. Today* **2002**, *72* (1−2), 51.
(15) Tabakova, T.; Boccuzzi, F.; Manzoli, M.; Andreeva, D. *Appl. Catal., A* **2003**, *252* (2), 385.
(16) Luengnaruemitchai, A.; Osuwan, S.; Gulari, E. *Catal. Commun* **2003**, *4* (5), 215.
(17) Tabakova, T.; Boccuzzi, F.; Manzoli, M.; Sobczak, J. W.; Idakiev, V.; Andreeva, D. *Appl. Catal., B* **2004**, *49*, 73.
(18) Sakurai, H.; Tsubota, S.; Haruta, M. *Catal. Catal. (Japanese)* **2002**, *44*, 416.
(19) Sakurai, H.; Akita, T.; Tsubota, S.; Kiuchi, M.; Haruta, M. *Appl. Catal., A* **2005**, *291* (1−2), 179.
(20) Guzman, J.; Carrettin, S.; Fierro-Gonzalez, J. C.; Hao, Y.; Gates, B. C.; Corma, A. *Angew. Chem. Int. Ed* **2005**, *44*, 4778.
(21) Si, R.; Flytzani-Stephanopoulos, M. *Angew. Chem., Int. Ed.* **2008**, *47*, 2884.
(22) Kim, C. H.; Thompson, L. T. *J. Catal.* **2005**, *230*, 66.
(23) Karpenko, A.; Leppelt, R.; Plzak, V.; Behm, R. J. *J. Catal.* **2007**, *252*, 231.
(24) Tabakova, T.; Boccuzzi, F.; Manzoli, M.; Sobczak, J. W.; Idakiev, V.; Andreeva, D. *Appl. Catal., A* **2006**, *298*, 127.
(25) Andreeva, D.; Ivanov, I.; Ilieva, L.; Sobczak, J. W.; Avdeev, G.; Tabakova, T. *Appl. Catal., A* **2007**, *333*, 153.
(26) Liu, Z.-P.; Jenkins, S. J.; King, D. A. *Phys. Rev. Lett.* **2005**, *94*, 196102.
(27) Jacobs, G.; Ricote, S.; Patterson, P. M.; Graham, U. M.; Dozier, A.; Khalid, S.; Rhodus, E.; Davis, B. H. *Appl. Catal., A* **2005**, *292*, 229.
(28) Tibiletti, D.; Amieiro-; Fonseca, A.; Burch, R.; Chen, Y.; Fisher, J. M.; Goguet, A.; Hardacre, C.; Hu, P.; Thompsett, D. *J. Phys. Chem. B* **2005**, *109* (47), 22553.
(29) Wang, X.; Rodriguez, J. A.; Hanson, J. C.; Pérez, M.; Evans, J. *J. Chem. Phys.* **2005**, *123*, 221101.
(30) Putna, E. S.; Vohs, J. M.; Gorte, R. J. *J. Phys. Chem.* **1996**, *100* (45), 17862119.
(31) Boulahouache, A.; Kons, G.; Lintz, H. G.; Schulz, P. *Appl. Catal., A* **1992**, *91*, 115.
(32) Li, C.; Domen, K.; Maruya, K. I.; Onishi, T. *J. Catal.* **1990**, *123*, 436.
(33) Li, C.; Chen, Y.; Li, W.; Xin, Q. *New Aspects of Spillover in Catalysis*; Inui T., et al., Eds.; Elsevier: Amsterdam, 1993; p 217.
(34) Long, R. Q.; Huang, Y. P.; Wan, H. L. *J. Raman Spectrosc.* **1997**, *28*, 53132.
(35) Deng, W.; Jesus, J. De.; Saltsburg, H.; Flytzani-Stephanopoulos, M. *Appl. Catal., A* **2005**, *291*, 126.
(36) Goguet, A.; Burch, R.; Chen, Y.; Hardacre, C.; Hu, P.; Joyner, R. W.; Meunier, F. C.; Mun, B. S.; Thompsett, D.; Tibiletti, D. *J. Phys. Chem. B* **2007**, *111* (45), 16927.
(37) Ravel, B.; Newville, M. *J. Synchrotron Rad.* **2005**, *12*, 537.
(38) Newville, M. *J. Synchrotron Rad.* **2001**, *8*, 322.
(39) Zabinsky, S. I.; Rehr, J. J.; Ankudinov, A.; Albers, R. C.; Eller, M. J. *Phys. Rev. B* **1995**, *52*, 2995.
(40) Frenkel, A. I.; Hills, C. W.; Nuzzo, R. G. *J. Phys. Chem. B* **2001**, *105* (51), 12689.
(41) Deng, W., Ph. D. dissertation, Department of Chemical and Biological Engineering, Tufts University, February, 2008.
(42) Machida, M.; Kurogi, D.; Kijima, T. *J. Phys. Chem. B* **2003**, *107*, 196.
(43) Akita, T.; Okumura, M.; Tanaka, K.; Kohyama, M.; Haruta, M., J. *Matet. Sci* **2005**, *40*, 3101.
(44) Romero-Sarria, Francisca.; Martý'nez, Leidy M.; Miguel, T.; Centeno, A.; Jose'; Odriozola, A. *J. Phys. Chem. C* **2007**, *111*, 14469.

JP800075Y